

Evaluation on structural behaviors of prestressed composite beams using external prestressing member

Jin-Hee Ahn, Chi-Young Jung and Sang-Hyo Kim[†]

School of Civil and Environmental Engineering, Yonsei University, Seoul 120-749, Korea

(Received August 6, 2009, Accepted November 20, 2009)

Abstract. In this study, experimental, numerical, and analytical approaches were carried out to evaluate the behavior and prestressing effect of prestressed composite beam by external tendon and cover plate. Behavior of prestressed composite beam, load-carrying capacity, effects of prestressing, and ultimate strength were estimated. The contribution of the section increase of the prestressing method using tendon was less than the prestressing method using cover plate. In accordance with numerical and analytical approaches, the ultimate strength of the prestressed composite beam is shown to be the same value because strength is determined according to the plastic resistance moment and the plastic neutral axis; however, both plastic resistance moment and neutral axis are not affected by prestressing force but affected by sectional stiffness of the prestressing member. Based on these approaches, we concluded that the prestressing method using tendon can be useful in applications without an increase in self-weight, and the prestressing method using high-strength cover plate can be applied to reduce the deflection of the composite beam. The prestressing method using high-strength cover plate can also be used to induce prestress of the composite beam in the case of a large deflection due to a smaller sectional stiffness of the composite beam.

Keywords: prestressing; prestressing member; load-carrying capacity; tendon; cover-plate; composite beam.

1. Introduction

Steel-concrete composite beams, prestressed with an external high-strength prestressing member, are known for their advantages over non-prestressed composite beams, which include elastic behavior under heavier loading, less deflection under service loading, improved fatigue strength and fracture behaviors, and higher crack resistance of the concrete slab at continuous beam under negative moment (Fisher and Wright 2001, Chen and Gu 2005, Lorenc and Hubica 2006). Therefore, the prestressing method can be adopted to improve the load-carrying capacity of the existing composite beams and composite girder bridges as a strengthening and retrofitting method and to improve the span length and sectional efficiency of new composite beams and composite girder bridges. To accomplish this, tendons are usually used as prestressing members externally or internally installed in the composite beams, composite girder bridges, and concrete bridges.

[†] Corresponding author, E-mail: sanghyo@yonsei.ac.kr

Recently, a new method which relies on thermal expansion and contraction of high-strength steel cover-plate prestressing has been proposed (Sakano *et al.* 2006, Ahn *et al.* 2009, Ahn *et al.* 2009a,b). This new prestressing method has several advantages compared to conventional prestressing methods using tendons: ease of obtaining a large prestressing force, minimization of stress concentration at the anchorage owing to distribution of the bolt connections, and contribution to structural stiffness by attached prestressing cover plates. In order to examine the behavior of the composite beam prestressed with prestressing members in the elastic range and the plastic range, experimental and theoretical studies were performed (Ahn *et al.* 2009).

In this study, to evaluate the prestressing effect and the behavior of prestressed composite beams as a consequence of the prestressing member and prestressing force, load-carrying capacity, effect of prestressing, and ultimate strength were estimated by conducting experimental, numerical, and analytical techniques on prestressed composite beams. Seven composite beam specimens were fabricated for the experimental approach. After the prestressing process and static-loading tests, the load-carrying capacities and behavior of the fabricated prestressed composite beam specimens were evaluated. The experimental results were then compared with the analytical results, which were obtained by FE analysis taking into consideration material nonlinearity and interaction between concrete slab and steel flange. Based on these comparisons the FE models were validated, and the effect on the prestressing force and the section increase of installed prestressing member for the prestressed composite beams were examined by the verified FE models.

2. Prestressing method using external prestressing member

There are currently two available methods for prestressed composite beams using external prestressing members. The prestressing methods using the prestressing tendon or cover plate are generally applied to improve the load-carrying capacity of the composite beam. The prestressing method using the cover plate, which is installed at the bottom flange in the pretensioned state, produces a prestressing force by a heating and cooling process. The prestressing method using tendons for the composite beam is used as shown in Fig. 1(a), where the tendons are installed on the upper or lower side of the bottom flange. Fig. 1(b) shows the method to induce prestressing by the cover plate. This prestressing method uses thermal expansion and contraction of the cover plate. It is similar to the method that uses prestressing tendons as members, but it is possible to adjust the prestressing force to multistep. In addition, the cover plate method can reduce the stress to the composite beam and deflections according to the increase of section properties affected by the attached cover plates (Ahn *et al.* 2009b). The general application procedure of the prestressing method using a cover plate (multi-stepwise TPSM) is shown in Appendix A and B.

The equations for the stresses in the bottom of the lower flange (f_{SL}), the top of the upper flange (f_{SU}), the bottom of the concrete slab (f_{CL}), and the top of the concrete slab (f_{CU}) can be easily obtained by dividing the prestressing force by the appropriate section properties given in Eq. (1) through (4), respectively, as shown in Fig. 2. The prestressing force is determined by the prestressing method. The prestressing method using tendons is dependent on the jacking force. The prestressing method using cover plates is dependent on the heating temperature of the cover plate, as shown in Eq. (5) (Ahn *et al.* 2009).

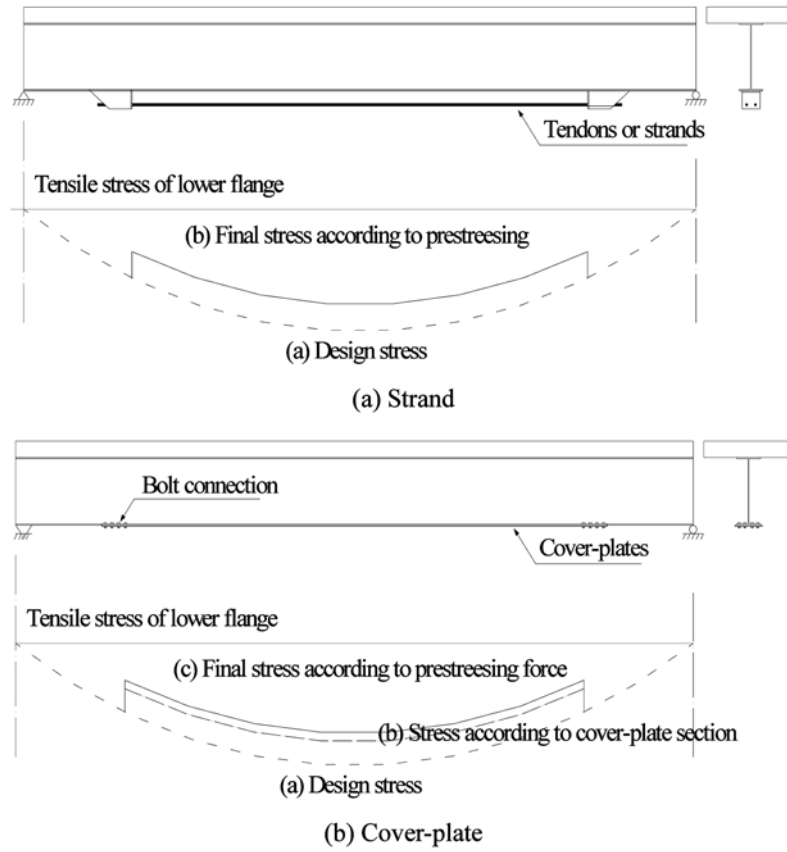


Fig. 1 Prestressing methods using external prestressing member (Ahn 2009)

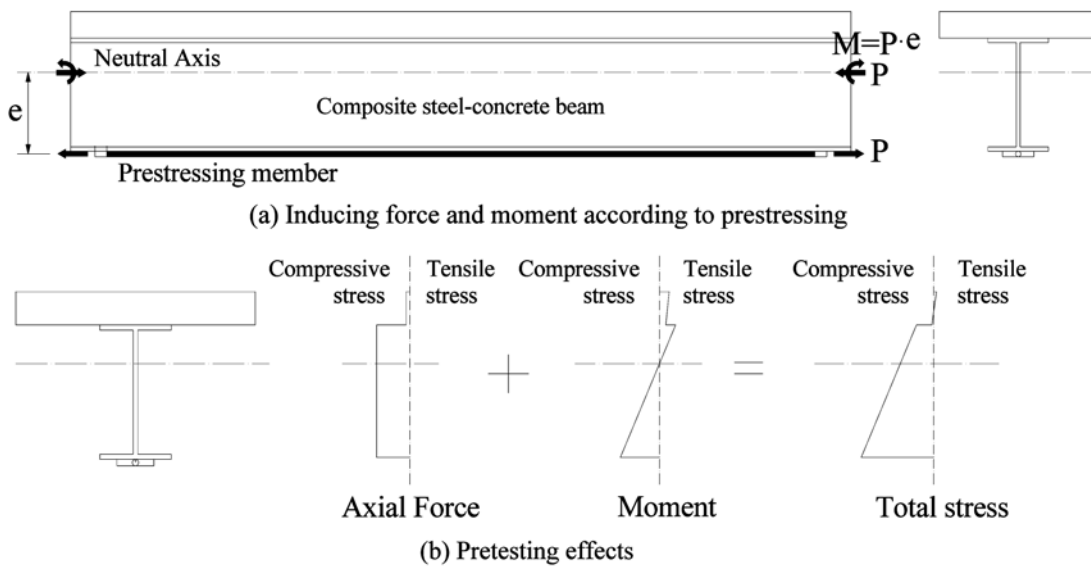


Fig. 2 Stress distribution of prestressed composite beam

$$f_{SL} = \frac{P_{TPSM}}{A_G} - \frac{P_{TPSM} \cdot e}{I_G} y \quad (1)$$

$$f_{SU} = \frac{P_{TPSM}}{A_G} + \frac{P_{TPSM} \cdot e}{I_G} (h_G - y) \quad (2)$$

$$f_{CL} = \frac{P_{TPSM}}{n \cdot A_G} + \frac{P_{TPSM} \cdot e}{n \cdot I_G} (h_G - y) \quad (3)$$

$$f_{CU} = \frac{P_{TPSM}}{n \cdot A_G} + \frac{P_{TPSM} \cdot e}{n \cdot I_G} (h_C + h_G - y) \quad (4)$$

$$P_{TPSM} = P_C = P_G = \frac{\alpha(\Delta T)EA_C A_G I_G}{A_G I_G + A_C I_G + A_C A_G e y} \quad (5)$$

where, P_{TPSM} is the prestressing force, e is the eccentric distance between the neutral axis of the composite beam and P_{TPSM} , h_G is the height of the steel girder, h_C is the thickness of the concrete slab, and y is the distance between the bottom of the lower flange and the neutral axis of the composite beam. A_G and I_G are the area and second moment of inertia of the steel girder, respectively, P_C is the prestressing force induced on the concrete slab of the composite beam, P_G is the prestressing force induced on the steel girder of the composite beam, A_C is the area of the concrete slab, α is the coefficient of thermal expansion of the cover plate, and E is the elastic modulus of the cover plate.

3. Static loading tests

3.1 Test specimens

To compare the behavior of a non-prestressed composite beam with prestressed composite beams with external prestressing members and to evaluate the prestressing effects on the composite beam according to the prestressing force and the prestressing member, a non-prestressed composite beam specimen, two composite specimens prestressed with tendons, and four composite specimens prestressed with cover plates were manufactured. The prestressing force and connection type of the prestressing member for each prestressed composite beam were changed to consider the effects on the load-carrying capacity and on sectional properties.

Table 1 and Figs. 3 and 4 show the characteristics and dimensions of prestressed composite beam specimens, depending on the prestressing members. All composite beams used the SS 400 grad hot-rolled beams having a 400-mm height and 200-mm width (H400 × 200 × 8 × 13); the concrete slab was designed as 1000 mm in width and 100 mm in thickness with 27 MPa compressive strength, as shown in Fig. 3. Head stud shear connectors were installed to have full shear connection in the composite beam, and they were uniformly distributed on the composite interface along the whole length of the beam, similar to the composite beam without prestressing (Ahn *et al.* 2009a,b). The dimension of the head stud shear connectors were 16 mm diameter and 80 mm height. A total of 56 shear connectors were installed.

Table 1 Layout of prestressed composite beam specimens

Specimens	Prestressing method	Prestressing force and heating temperature	Connection	Remarks
SC-C00	-	-	-	-
SC-C00-S140	External strand	140 kN	Anchorage	15.2mm diameter strand
SC-C00-S180	External strand	180 kN	Anchorage	15.2mm diameter strand
SC-C10-WC	External cover-plate (TPSM)	30-50-30°C	Bolting & welding	10 mm thickness cover-plate
SC-C12-WC	External cover-plate (TPSM)	30-50-30°C	Bolting & welding	12 mm thickness cover-plate
SC-C10-BC	External cover-plate (TPSM)	30-50-30°C	Bolting	10 mm thickness cover-plate
SC-C12-BC	External cover-plate (TPSM)	30-50-30°C	Bolting	12 mm thickness cover-plate

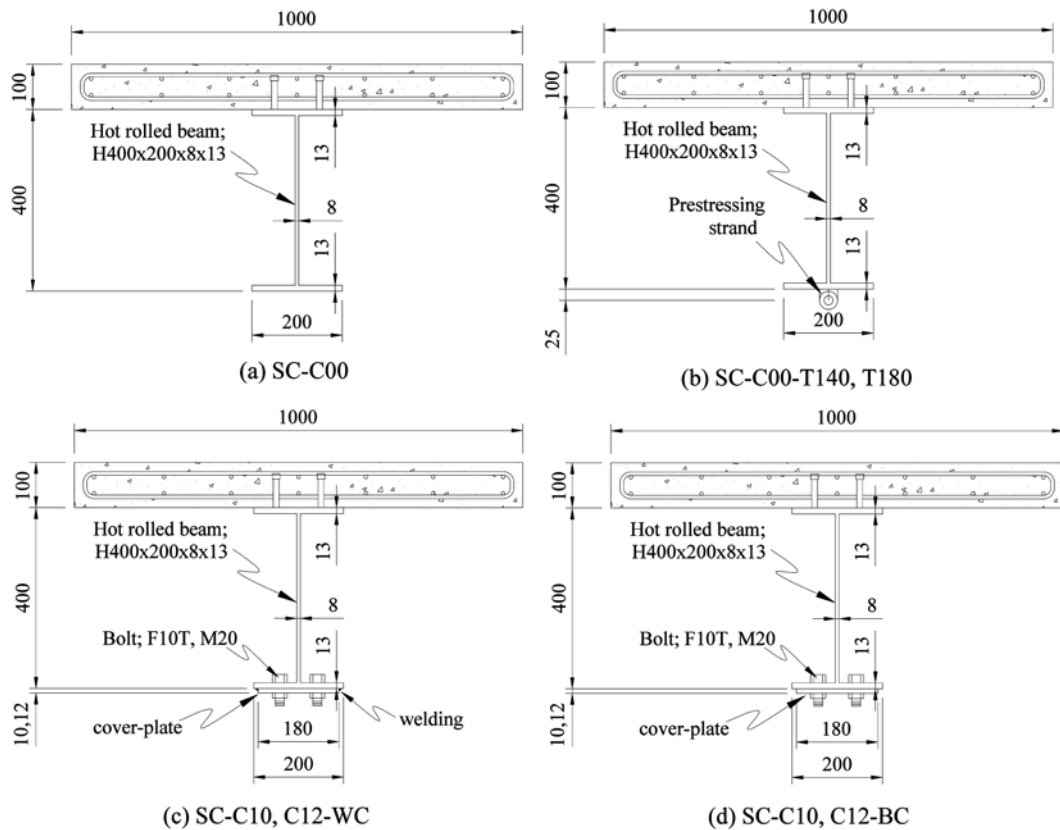


Fig. 3 Cross section of specimen (unit: mm)

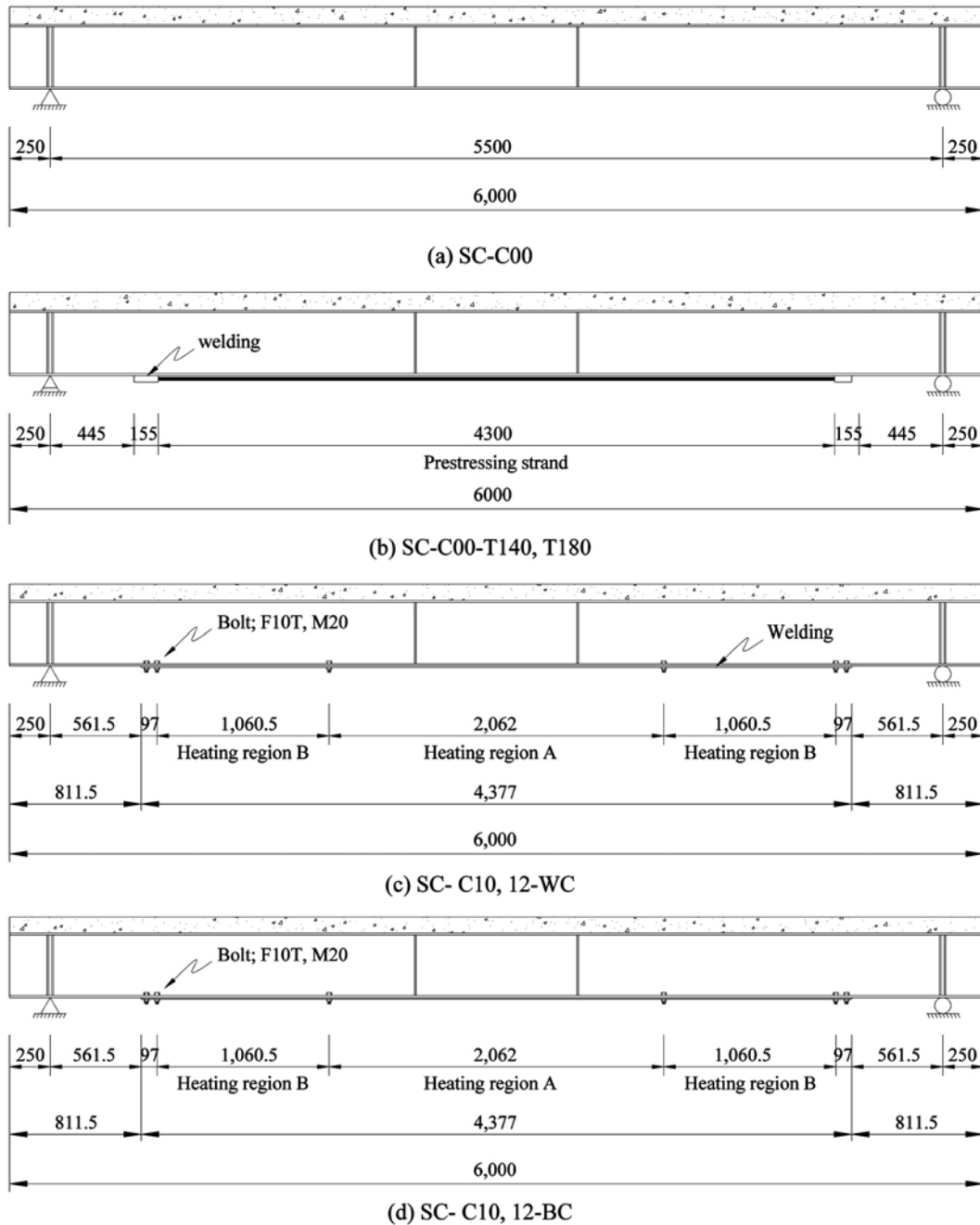


Fig. 4 Elevations of specimen (unit: mm)

In Table 1, in the case of the composite beam specimen, SC is the steel-concrete composite section, C00, 10, 12 are the thickness of the cover plate, and S, WC, BC are the tendon, welded, and bolted connection, respectively. The SC-C00 specimen was fabricated to compare the contribution of the prestress and prestressing member to the sectional rigidity in the composite

beam. The SC-C00-T140 and T180 specimens were composite beams prestressed with tendon, the SC-C00-T140 specimen was induced with 140 kN prestressing force, and the SC-C00-T180 specimen was induced with 180 kN prestressing force by a hydraulic jacking system. The anchorages of the prestressing tendons were installed on the bottom exterior side. Seven-wire PC Strand (SWPC7B) was used as the prestressing member in the composite beam.

Other composite beam specimens were prestressed with the high-strength cover plate to which thermal expansion was applied, and the elastic thermal deformation energy was converted to prestressing force by a temporary heating process of the cover plate (the cover plate was cooled after the heating process). SC-C10-WC and SC-C12-WC specimens were prestressed with a cover plate of 10 mm and 12 mm thickness and 180 mm width before casting the concrete slab. The length of the cover plate was 4377 mm. Prestress is achieved by thermal stresses through preheating and subsequent cooling of the cover plate. In Fig. 4 the temperature of the heating region A was 50°C and that of region B was 30°C after thermal equilibrium was reached in the heated cover plate. When there was no further temperature change, the cover plate was connected to the rolled beam using high tension bolts (F10T, M20). After the bolting was completed, the heaters were removed and the contraction behavior of the cover plate, as it cooled, induced prestress in the rolled beam. By differentiating the heating temperature in each heating region, the multi-stepwise prestress force can be induced to the rolled beam. The cover plate was welded to the rolled beam by fillet welding along the plate length. The concrete slab was then casted after welding was finished. The bolts were not removed after welding. SC-C10-BC and SC-C12-BC specimens were prestressed using a cover plate of 10 mm and 12 mm thickness and 180 mm width. After curing the concrete slab, the multi-stepwise heated cover plate and the lower flange of the composite beam were connected using high-tension bolts; a multi-stepwise prestress force was induced to the composite beam.

3.2 Material properties of specimens

The rolled beam for the composite section was made of SS400 grade steel, which has 140 MPa in allowable stress and 240 MPa in nominal yield strength. The concrete slab was designed with 27 MPa compressive strength and a maximum grade of 25 mm and a slump of 120 mm. In the prestressing method using tendon, the seven-wire strand was used. In the prestressing method using a cover plate, SM520 (10-mm cover plate) and SM570 (12-mm cover plate) steel grade were used.

Table 2 Material properties of steel

Steel grade	Nominal strength		Tensile strength test		
	Allowable (MPa)	Yield (MPa)	Yield (MPa)	Tensile (MPa)	Elongation (%)
SS400	140	240	253	476	24
SM520	210	360	381	595	23
SM570	260	460	476	681	23

Table 3 Material properties of PC strand

Classification mark	Standard diameter (mm)	Nominal area (mm ²)	Yielding strength (kN)	Load caused by 0.2% permanent elongation
SWPC7B (seven-wire)	15.2	138.7	260.68	221.48

Table 4 Material properties of concrete

	Design strength (MPa)	28 days; standard curing (MPa)	Static loading (MPa)
Compressive strength	27	28.3	29.3

Before the fabrication of the composite beam, a tensile strength test of steel and a compressive strength test of concrete were conducted to determine the material properties of the composite specimens (Tables 2, 3, and 4).

3.3 Test program and instrumentation

The prestressed composite beam specimen tests were carried out as follows: First, prestress was induced to the composite beam specimens depending on the type of prestressing member. After prestressing and fabrication of the composite beam, static loading tests were carried out with a displacement-controlled MTS actuator system of 1000 kN capacity.

For the SC-C00-T140/T180 specimens prestressed with tendon and SC-C10/12-BC specimens prestressed with cover plate, prestress was induced after the concrete slab was cured. When prestress was induced, a 28-day compressive strength was achieved (tested with a concrete cylindrical test). In contrast, for the SC-C10/12-WC specimens prestressed with cover plate, prestressing was induced before the concrete slab was cast and the cover plate was welded on the steel beam after the cover plate had completely cooled. Fig. 5 shows the prestressing process of the

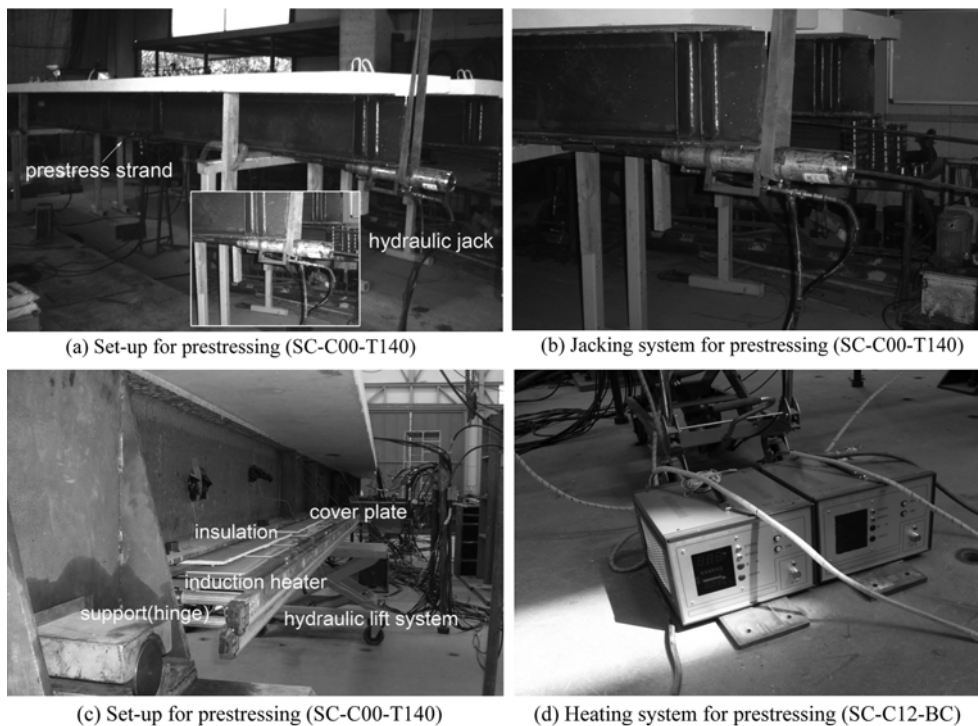


Fig. 5 Prestressing process of composite beam

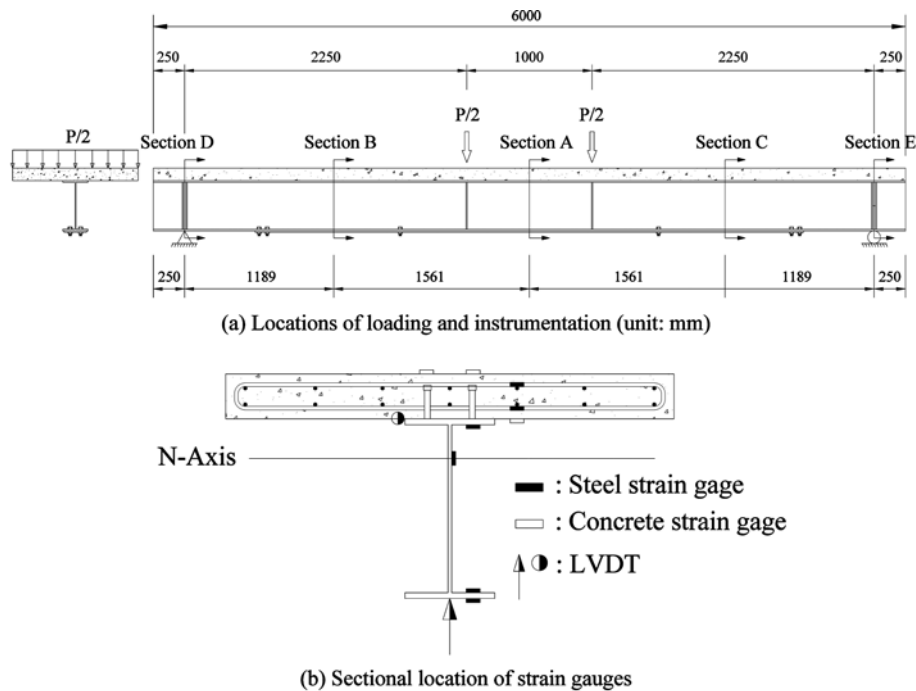


Fig. 6 Locations of loading and instrumentation (unit: mm)

composite beam.

The static loading tests on the composite beams used two-point loading spaced 1000 mm apart (Fig. 6); displacement increments were 2 mm/min. The static loading tests were controlled with displacement to avoid the sudden failure of specimens. In this research ultimate state could not be conducted because of the safety problems, such as specimen turn over and break down of external prestressing member.

For each measurement section of each specimen (cross-sections A, B, C, D, and E), five steel strain gauges on the steel beam and three concrete gauges on the concrete slab were mounted and two steel gauges were mounted on the rebar embedded in the concrete slab. The three linear variable differential transforms (LVDTs) were installed to measure the load-deflection relationships at the central cross-section (cross-section A) and its exterior cross-section (cross-sections B and C). Additionally, the relative slips on the composite interface were measured at cross-sections A, B, C, D, and E between the concrete slab and the steel beam by installing the LVDT.

4. Static loading test results

4.1 Prestresses

Fig. 7 presents the induced prestresses and deflections of the composite beam specimens by the prestressing process according to hydraulic jacking of the tendon and heating of the cover plate, before the loading test. Compressive strains and tensile strains were induced in the upper slab and

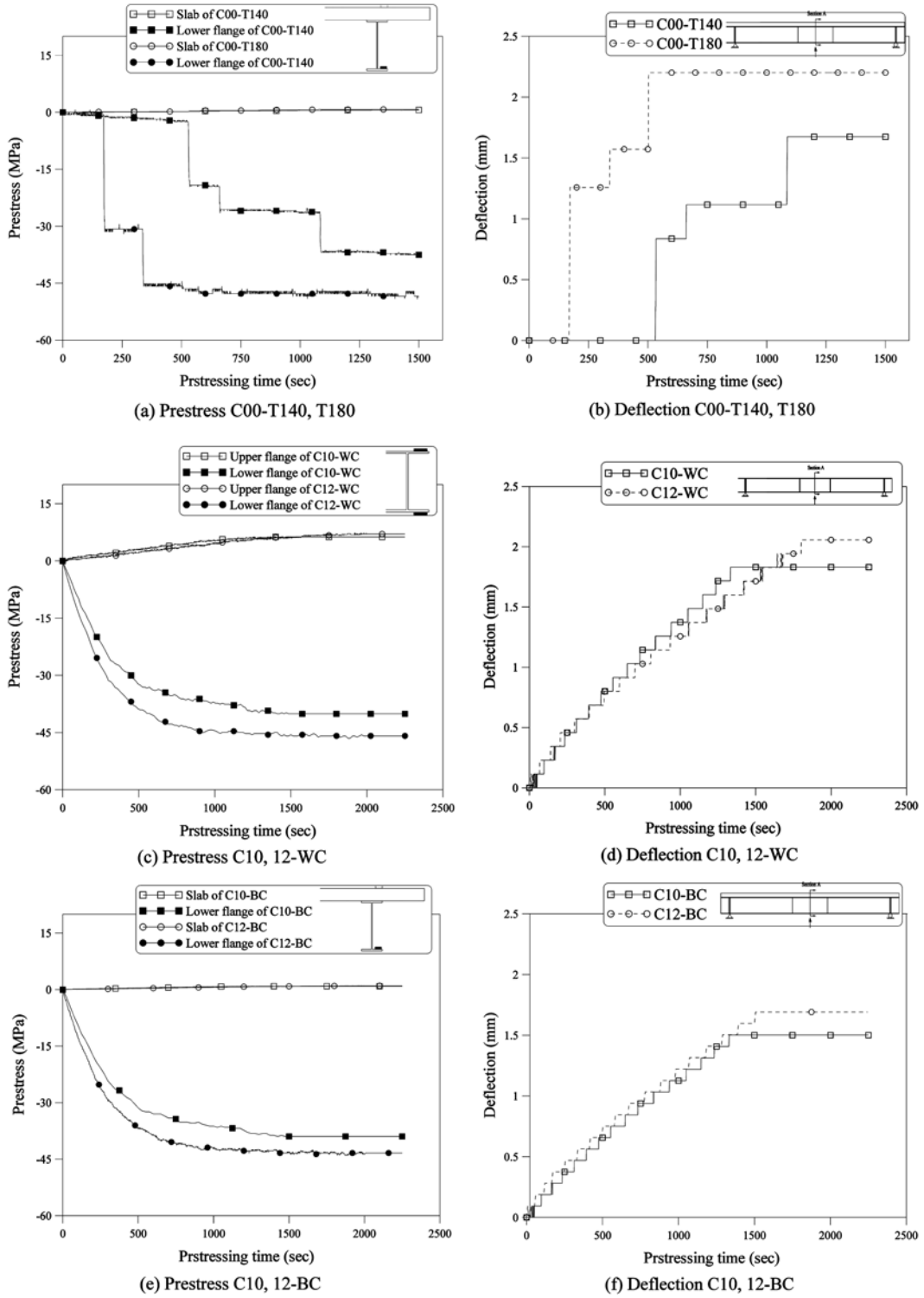


Fig. 7 Induced prestresses and deflections

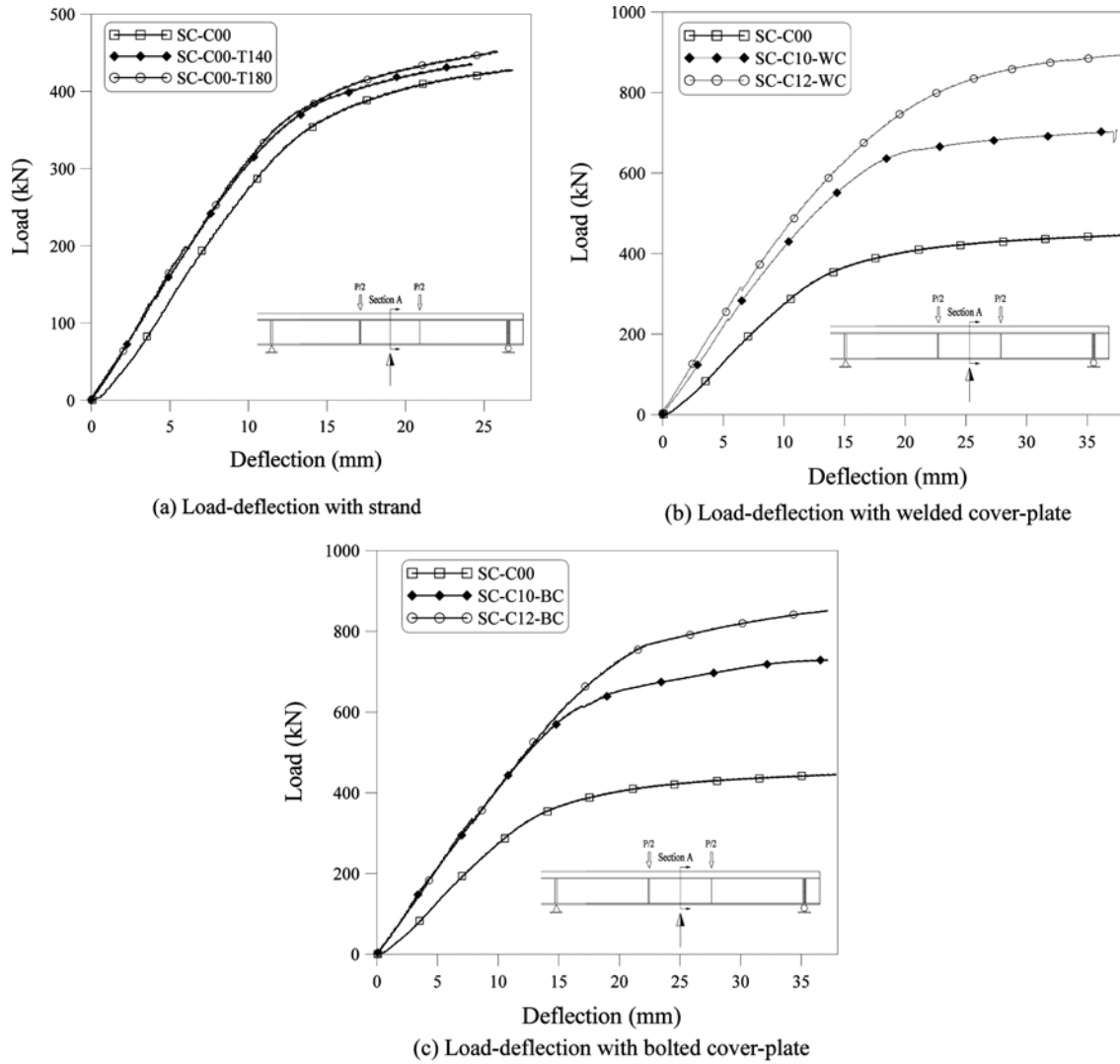


Fig. 8 Load-deflection curves of the prestressed specimens

Table 5 Static loading test results

Specimens	Yield load (kN)	Yield load ratio	Stiffness (kN/mm)	Stiffness ratio
SC-C00	320.69	1.00	26.01	1.00
SC-C00-T140	371.02	1.16	26.26	1.01
SC-C00-T180	382.04	1.19	27.21	1.05
SC-C10-WC	564.18	1.76	36.97	1.42
SC-C12-WC	611.77	1.91	40.33	1.55
SC-C10-BC	568.35	1.77	36.43	1.40
SC-C12-BC	605.87	1.89	39.29	1.51

flange and lower flange by eccentric axial force developed according to the prestressing force (Fig. 7). The results of Fig. 8 and Table 5 were measured at the center of the composite beam (Section A).

In the case of the SC-C00-T140/180 specimen prestressed to 140 and 180 kN using hydraulic jacking, tensile stresses of 0.81 and 1.78 MPa were induced in the top of the slab and compressive stresses of -37.51 and -48.24 MPa were induced in the lower side of the bottom flange; an upward deflection of 1.67 and 2.20 mm occurred as shown in Figs. 7(a) and (b).

In the case of the SC-C10/12-WC and SC-C10/12-BC specimens prestressed with cover plate, the heating process of the cover plate was completed using an electric heater and the connection process was completed using high tensioning bolting. Then as cover plate cooled down, the multi-stepwise thermal prestress in the specimens was induced by the contraction behavior of the cover plate. For SC-C10/12-WC specimens prestressed before casting the concrete slab, the tensile stresses of 6.28 and 7.18 MPa were induced in the upper side of the top flange and the compressive stresses of -40.14 and -45.95 MPa were induced in the lower side of the bottom flange on each specimen. As shown in Figs. 7(c) and (d) for SC-C10/12-BC specimens, the tensile stresses of 0.89 and 1.01 MPa were induced in the upper side of the top flange and the compressive stresses of -40.15 and -45.16 MPa were induced in the lower side of the bottom flange. An upward deflection of 1.83, 2.06, 1.50, and 1.69 mm occurred on each specimen, similar to prestressing using hydraulic jacking, as shown in Figs. 7(d) and (f).

4.2 Static loading tests

Fig. 8 presents the load-deflection curves of the prestressed composite beam, depending on prestressing force and prestressing member under static loading, compared with that of a non-prestressed composite beam. The shapes of the load-deflection curves in all composite beam specimens were similar (Fig. 8). The load-deflection relationships of composite beams were linear in the elastic region, whereas the load-deflection relationships changed nonlinearly after yielding in the lower flange of the composite beam specimens. Cracks were initially observed at the concrete slab, and these were propagated into the lower parts of the slab as the static loading level increased. All of the crack patterns of the initial concrete slabs were shown to be slightly slanted to the installed head studs. The cracks appeared in the composite interface of the concrete slab at the ends of the prestressed composite beams as a result of the flexible behaviors of the composite beam specimens, as shown in Fig. 10.

In the prestressed composite beams with tendon, the deflections of the composite beam specimens increased with increasing loading level, whereas the gap between the lower flange and tendon decreased.

In the prestressed composite beams with cover plate, the cover plate for prestressing acted as a single unit with the composite beam due to the bolted and welded connection.

A comparison of SC-C00 and SC-C00-T140/180 is shown in Fig. 8(a). The load-deflection curve of SC-C00-T140/180 was stiffer than that of SC-C00 and its yield loads were about 30 kN higher than SC-C00. The yield load of SC-C00-T180 was higher than that of SC-C00-T140.

As shown in Figs. 8(b) and (c), the stiffness of SC-C10/12-WC and SC-C10/12-BC were highly increased, and yield loads of the prestressed composite beam with cover plate increased up to about 530-570 kN. With an increase in the thickness of the cover plate, the yield loads of SC-C12-WC/BC increased despite having the same heating temperature. This is because the traction force

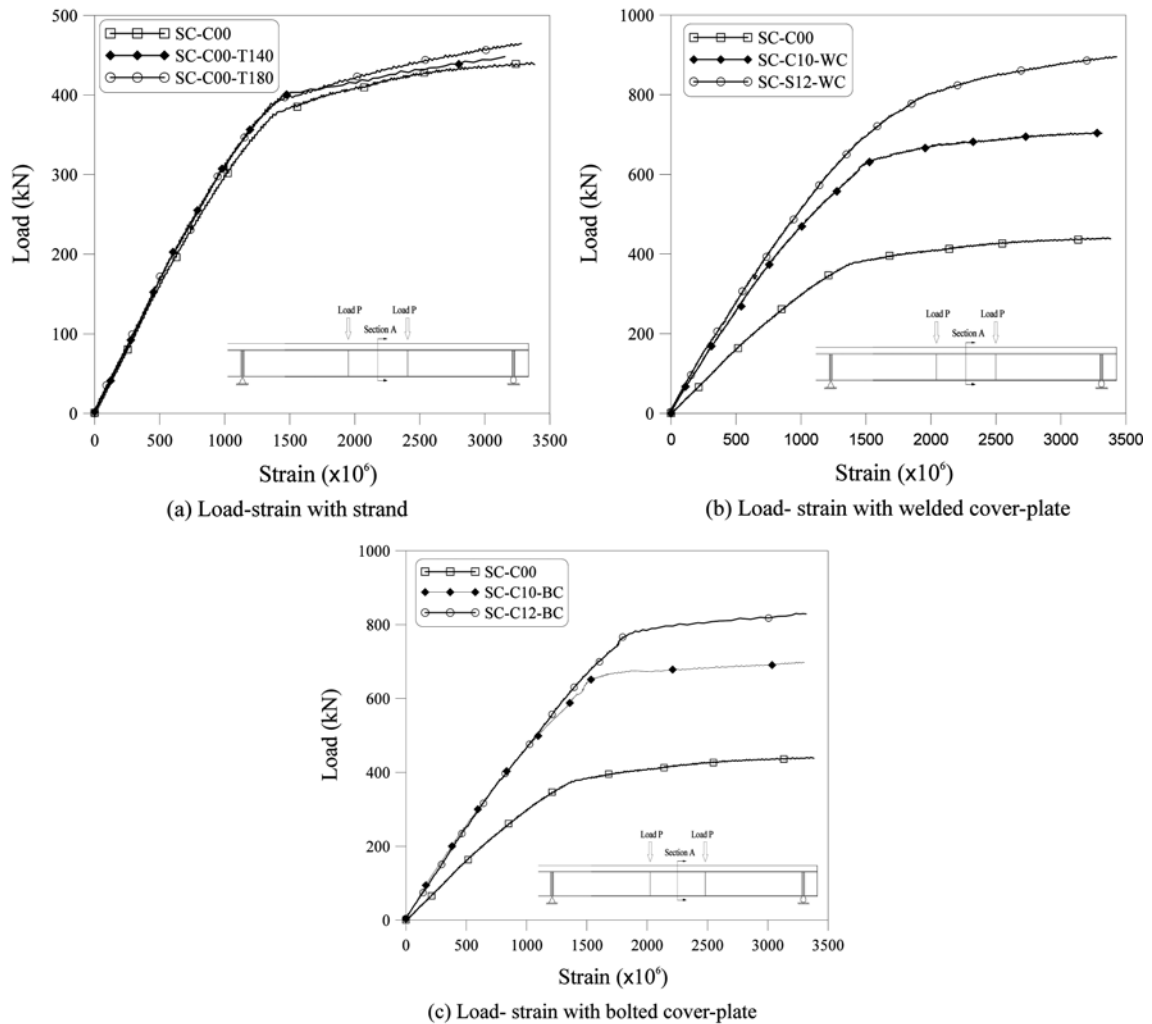


Fig. 9 Load-strain curves of the prestressed specimens

developed from the cooling of the heated cover plate (thermal prestressing force) and sectional properties of the composite beam are in proportion to the cross-sectional area of the cover plate. In addition, for SC-C10/12-WC, its yield loads were larger than those of SC-C10/12-BC because the welding of the beam and cover plate cause them to act as a single section.

Fig. 9 shows the load-strain relationship of the prestressed composite beam compared to the non-prestressed composite beam. The strain variations of the specimens were similar to the deflection variations according to the increase in the load. Fig. 10 illustrates the strain distribution in section A, indicating the typical tensile and compressive strain distribution. The yield strength of prestressed specimens were less than that of a non-prestressed composite specimen owing to the induced prestress and the change of section properties such as neutral axis and section modulus, which are similar to the load-deflection and strain relationship. Fig. 11 shows the load-relative slip relationship on the composite interface. The relative slips of the all composite specimens were small in the linear range, but the relative slips of the prestressed composite beam with cover plate were

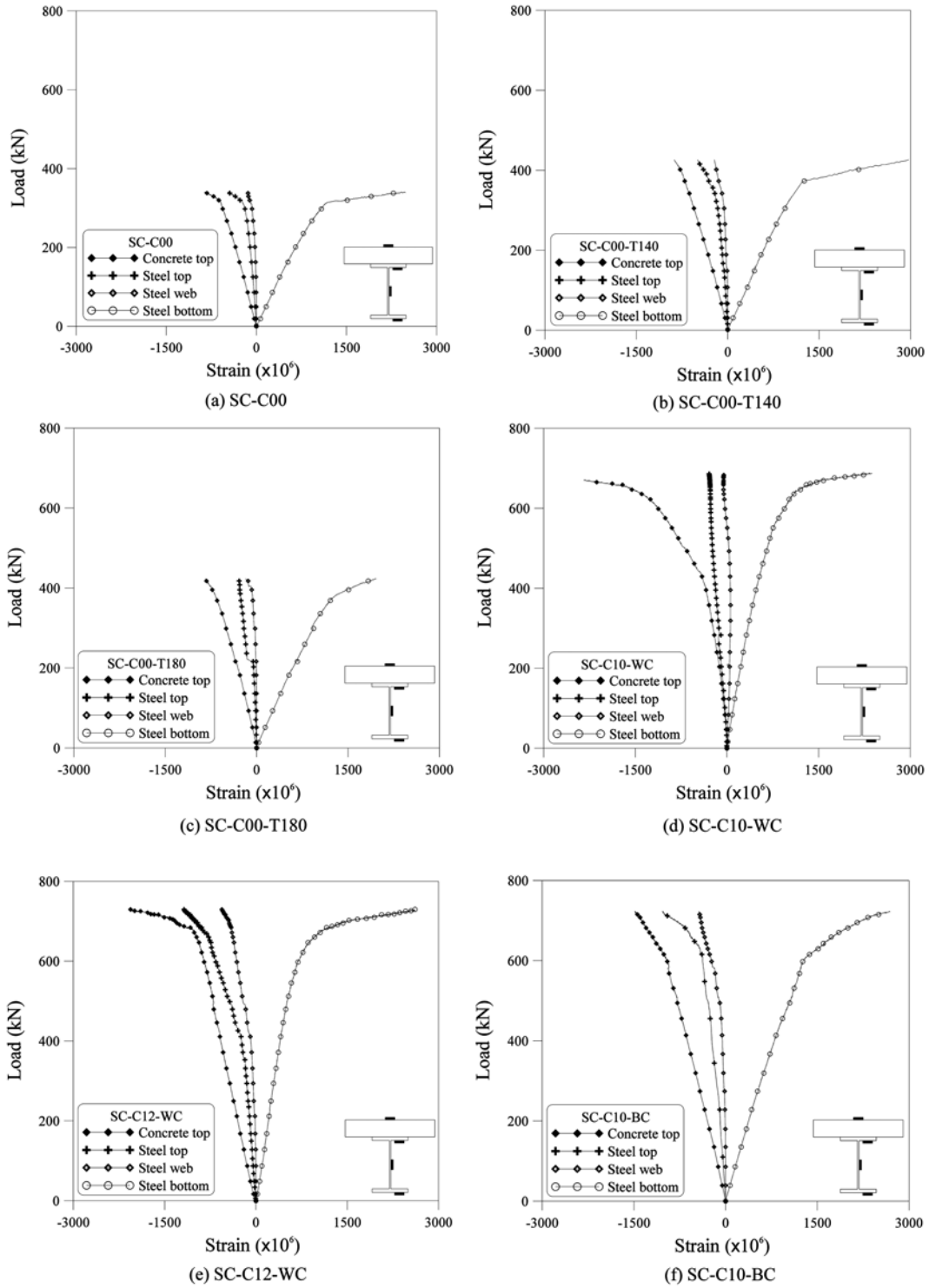


Fig. 10 Strain distributions in the section A

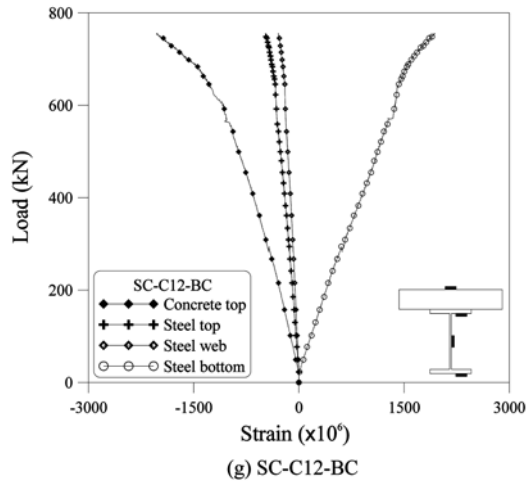


Fig. 10 Continued

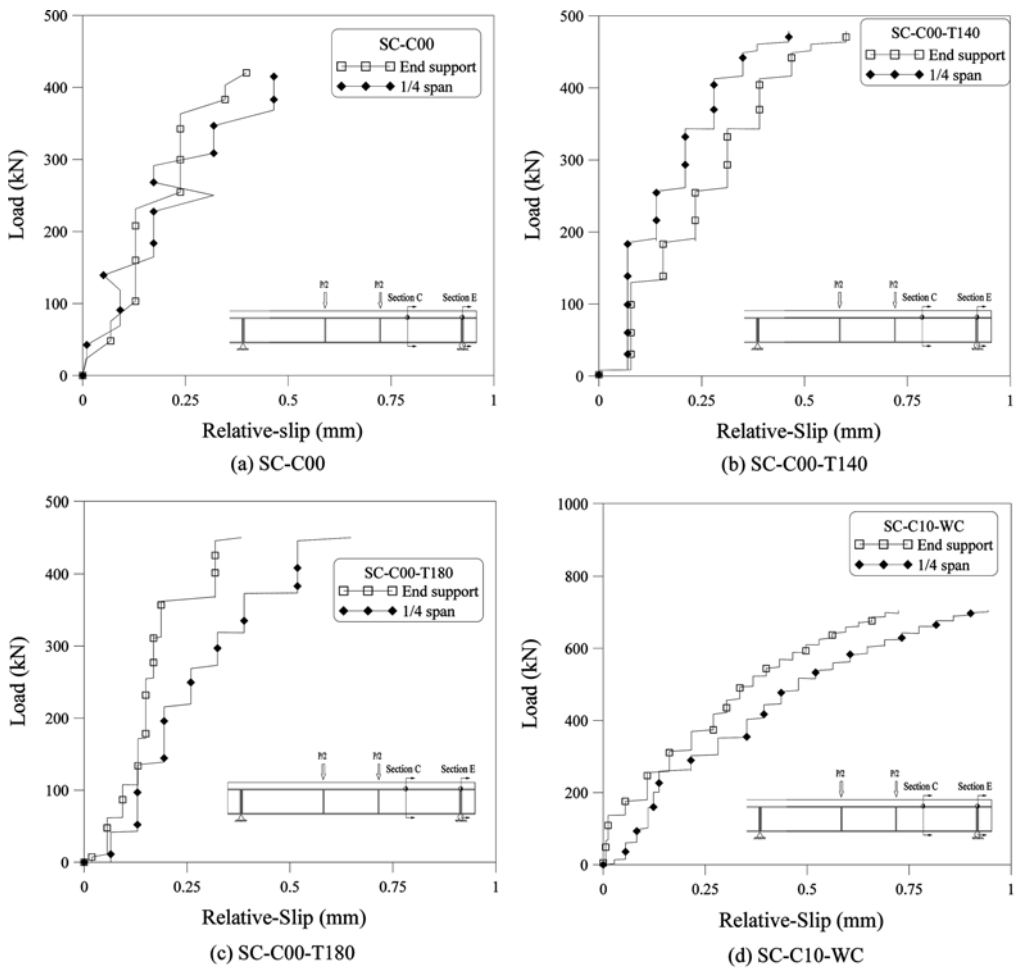


Fig. 11 Load-relative slip curves of the prestressed specimens

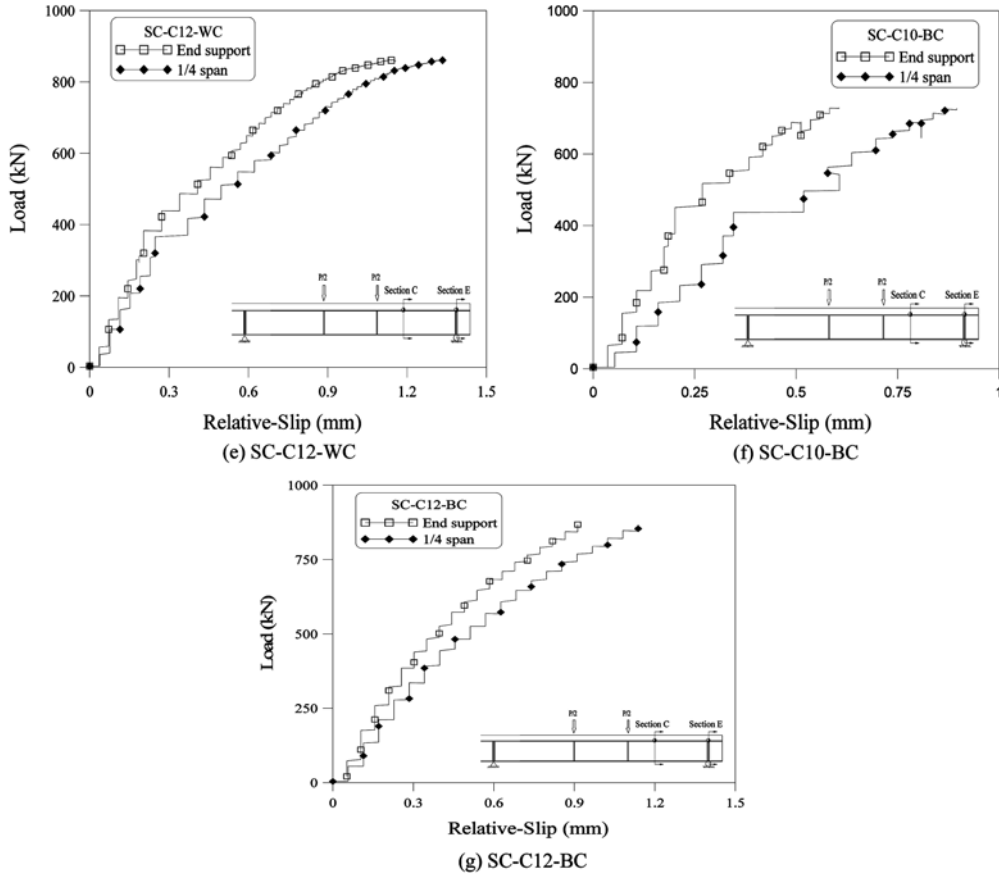


Fig. 11 Continued

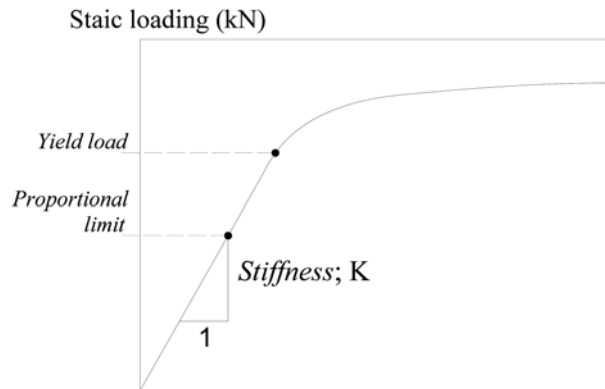


Fig. 12 Definition of yield load and stiffness

more sharply increased at higher load levels when the load levels became strongly nonlinear. This was because head stud shear connectors were installed to have full shear connection in composite beams without installing the prestressing member.

Table 5 summarizes the comparison of the yield load and stiffness of each prestressed composite

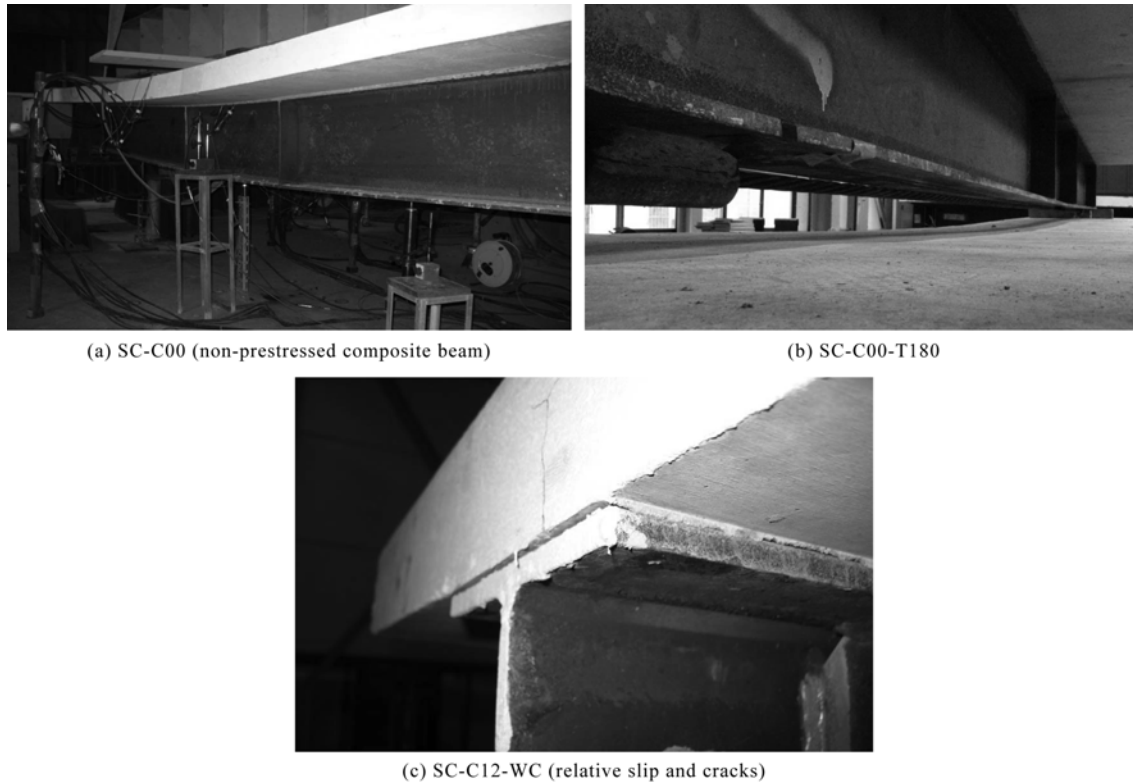


Fig. 13 Prestressed composite beam specimens after loading test

beam specimen. The yield load and stiffness of the specimens were defined as the strain on the lower flange at the center section equal to the yield strain, as shown in Fig. 12. In this study, the yield load could not be achieved by the 0.2%-offset strain method because the loading tests were not conducted until the ultimate state of the specimens. A definition of the yield load, therefore, is the load when the lower flange yielded.

In Table 5, the yield loads of the SC-C00-T140 and T180 specimens prestressed with tendon increased by 16~19% and their stiffness by 1~5% compared to SC-S00 specimens without prestressing. The yield loads of the SC-C10-WC and SC-C12-WC specimens prestressed with cover plates increased by 76~91% and their stiffness by 42~55% compared to SC-S00 specimens without prestressing. In addition, for the SC-C10-BC and SC-C12-BC specimens whose cover plates and composite beams were connected with bolts, their yield load increased by 77~89% and their stiffness by 40~51% compared to SC-C00 specimens without a prestressing member.

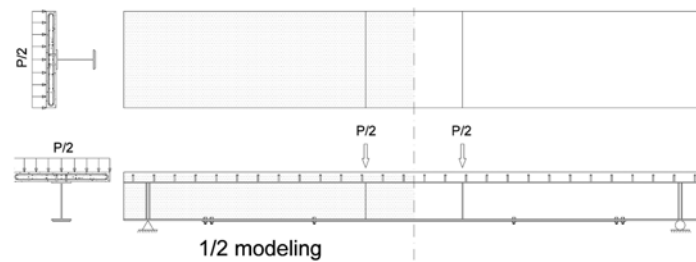
Thus, prestressing the composite beam using the prestressing member under service loading increases the stiffness and yield load of the composite beam to achieve an increase in the load-carrying capacity and reduction in the deflection of the composite beam. Fig. 13 shows the relative slip and cracks in prestressed composite beam specimens.

4.3 Comparison of experimental results with FE analysis results

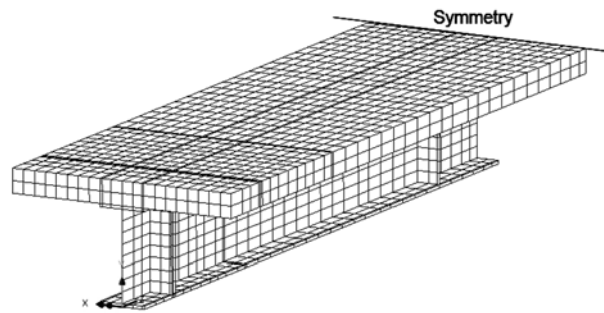
An FE analysis study was carried out using LUSAS 14. Two different types of models were used.

Table 6 Stiffness of stud shear connector resulted from push-out tests

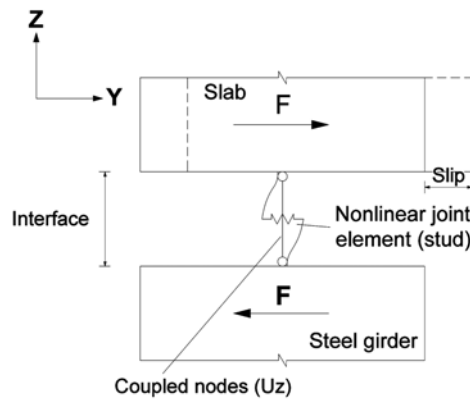
Specimen	Elastic spring stiffness			Strain hardening stiffness		
	P_e (kN)	S_e (mm)	K_e (kN/mm)	P_u (kN)	S_u (mm)	K_p (kN/mm)
ST-S-A1	48.70	0.63	77.31	97.41	8.66	6.07
ST-S-A2	50.28	0.49	102.61	100.56	7.64	7.03
ST-S-A3	48.94	0.53	92.35	97.89	9.12	5.70
Avg.	49.31	0.55	90.76	98.62	8.47	6.27



(a) Prestressed composite girder model, 3D-1/2



(b) Modeling, 3D half modeling



(c) The shear connector model (Queiroz *et al.* 2007)

Fig. 14 FE model of prestressed composite beam

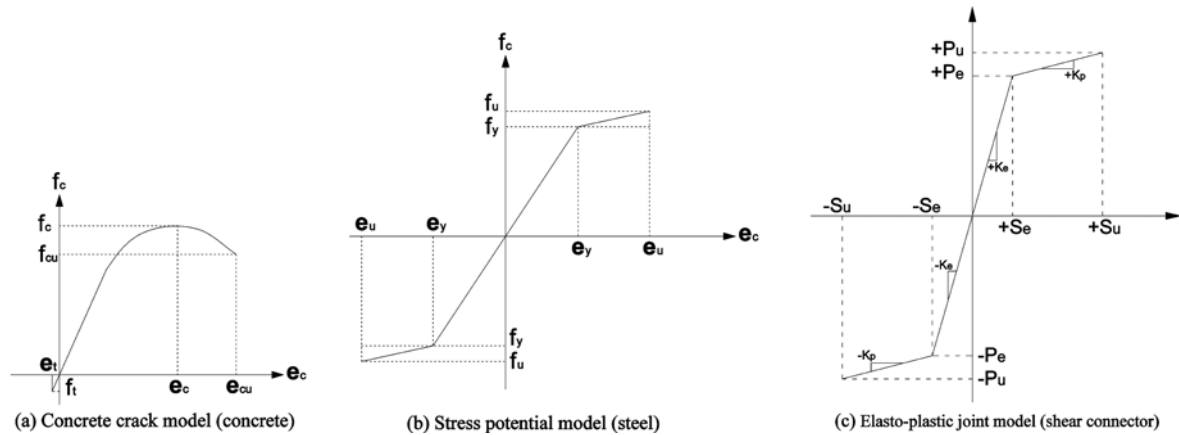


Fig. 15 Stress-strain relationship of the materials

One was a full interaction (FI) model, while the other was a partial interaction (PI) model. In the FE analysis, the solid element HX20 was assigned for the concrete slab, the steel beam flanges, and the external prestressing member. The surface element QSL8 was assigned for the steel beam web. In the PI model, the elasto-plastic joint element JNT4 as stud shear connectors was applied to the interaction between steel flange and concrete slab (Queiroz *et al.* 2007, Ahn *et al.* 2009b, Ranzi and Bradford 2009). The load-relative slip curves for the studs were based on a table of shear force and relative slip data, which were used as the inputs for the nonlinear springs for the longitudinal and lateral stud shear stiffness according to the push-out test results (Table 6). The rigid joint element as the vertical shear stiffness was used to prevent overlap of the concrete and steel elements. It is assumed in the tendon model that the gap between the lower flange of the steel beam and tendon remains constant. Due to the symmetrical nature of the problem, only the left-hand span of the beam is modeled. In its application, the load should be distributed incrementally in the model. Fig. 14 shows the FE model of the prestressed composite beam. Additionally, nonlinear material properties were assigned to consider the effect of material nonlinearity on structural behavior of the composite beam. Stress potential for steel material and the concrete crack model for the concrete material were assigned to plastic properties of the models. The results from the tensile and compressive test for the static loading test were applied to the material properties in the FE analysis model. Fig. 15 shows the plastic material characteristics.

Fig. 16 shows the load-deflection relationship, which compares the analytical results of the FI and PI models with the experimental results. Based on the analytical results, we conclude that the initial elastic stiffness of the FI models from the load-deflection curves are greater than those of the PI models and experimental results. In the case of the PI model, the load-deflection curve is quite similar to the experimental results. Table 7 presents the yield load and deflection of the composite beam after comparing differences between the FE models and experiments. The differences of the FI models are 1.33~4.45% in yield load and 6.20~13.83% in deflection, and those of the PI models are 0.89~1.48% in yield load and 0.30~4.49% in deflection. It can therefore be concluded that the composite beam behaves similar to a partial shear connection even if it was designed as a full shear connection. The PI model was validated by these results and a good agreement was obtained.

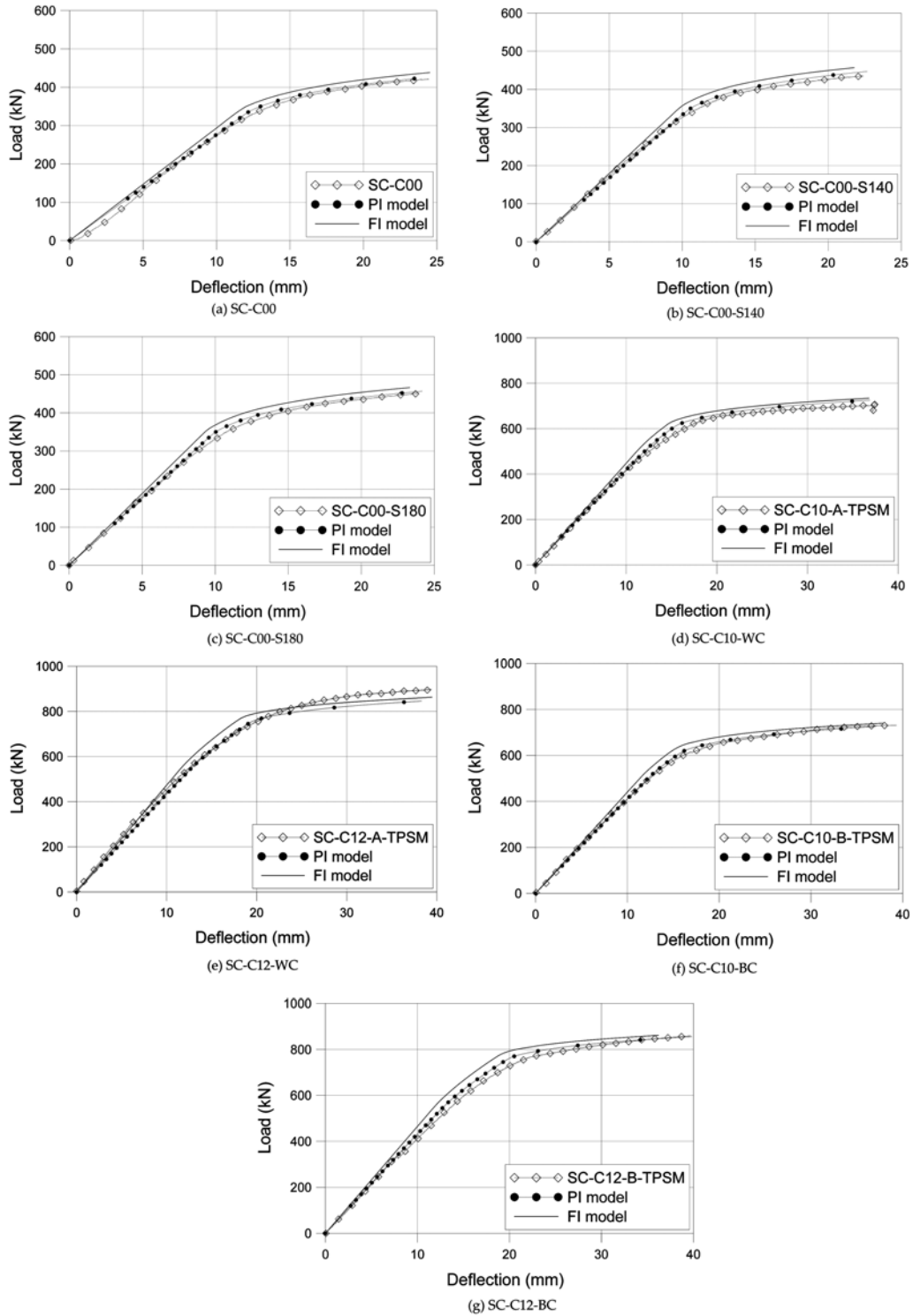


Fig. 16 Load-deflections comparison with FI model

Table 7 (a) Yield load of FE model

Specimens	Test	FI model	Error (%)	PI model	Error (%)
SC-C00	320.69	334.95	4.45	317.83	0.89
SC-C00-T140	371.02	375.96	1.33	368.86	0.58
SC-C00-T180	382.04	388.31	1.64	377.02	1.31
SC-C10-WC	564.18	588.98	4.40	561.56	0.46
SC-C12-WC	611.77	633.49	3.55	604.29	1.22
SC-C10-BC	568.35	586.12	3.13	559.92	1.48
SC-C12-BC	605.87	629.17	3.85	601.84	0.67

(b) Deflection at yield load of FE model

Specimens	Test	FI model	Error (%)	PI model	Error (%)
SC-C00	12.33	11.39	-7.62	12.60	2.19
SC-C00-T140	14.85	13.47	-9.29	15.01	1.04
SC-C00-T180	14.04	13.17	-6.20	14.67	4.49
SC-C10-WC	15.26	13.29	-12.92	15.31	0.30
SC-C12-WC	15.17	13.52	-10.88	15.57	2.66
SC-C10-BC	15.60	13.44	-13.83	15.48	0.74
SC-C12-BC	15.42	13.63	-11.61	15.70	1.82

5. Evaluation of the prestressing effect of the prestressed composite beam

From the experimental results of the prestressed composite beam specimens, we confirmed that prestressing the composite beam increases the stiffness and yield load of the composite beam. However, the effect of prestressing on the composite beam with cover plate is ambiguous because the yield load of the composite beam can be increased by attaching the cover plate without heating (without thermal prestressing), and the same applies to the prestressed composite beam with tendon. Therefore, an FE parametrical study was carried out to evaluate the prestressing effect of the prestressed composite beam with an external prestressing member.

In the case of the FE analysis model of the prestressed composite beam with tendon, the prestressing force was changed to evaluate the prestressing effect. Generally, the flexural rigidity of the tendon is disregarded since the area of the tendon is very small compared to the area of the composite beam. The load-carrying capacity and stiffness of the composite beam can be affected, however, by the sectional properties and material properties of the tendon. Therefore, the load-carrying capacity of the composite beams prestressed with prestressing forces of 180 kN, 360 kN, and 540 kN were compared with both a composite beam without a tendon and a composite beam with a tendon but which was not tensioned.

In the case of the FE analysis model of the prestressed composite beam with cover plate, the temperature distributions of the cover plate were determined as 30-50-30°C, 60-100-60°C, and 90-150-90°C. The connections of the cover plates and composite beams were considered as bolted connections in order to evaluate the prestressing effect based on the change in the temperature distribution of the cover plate; the welded connection case was not applied. The 12-mm thick cover plate was used.

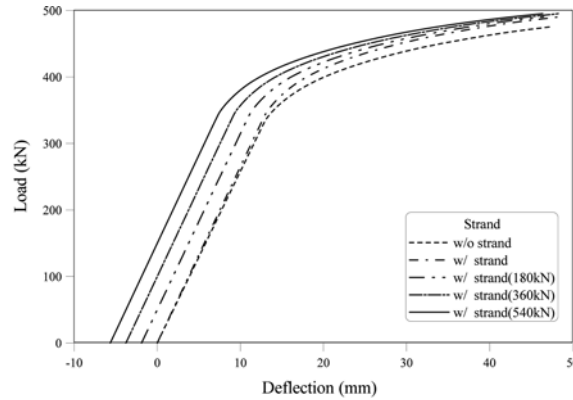


Fig. 17 Load-deflection curves of the strand case from FE analysis results

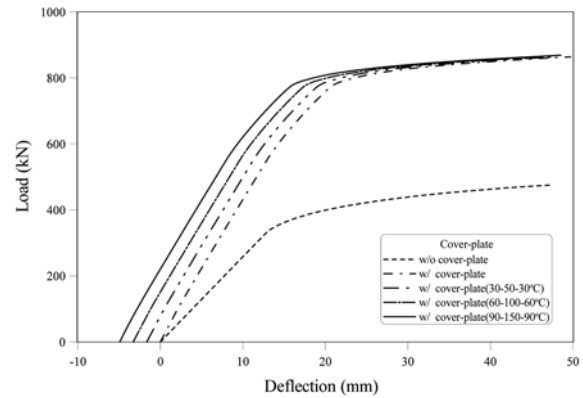


Fig. 18 Load-deflection curves of the cover-plate case from FE analysis results

Figs. 17 and 18 present the load-deflection curve of the prestressed composite beam from the FE analysis. The load-deflection relationships of the composite beams, regardless of the prestressing force and the prestressing member, throughout the entire range of loading up to the ultimate strengths of the composite beams, are shown in Figs. 17 and 18. In each case, the behavior of the prestressed composite beam was initially linear. After the first yielding of the bottom flange, the behavior was shown to be gradually nonlinear as the yielding of the steel beam progressed into the flange and the web, similar to the behavior of the tested prestressed composite beam, as shown in the experimental results.

From the load-deflection curves of the prestressed composite beam with tendon in Fig. 17, the stiffness and yield loads of the prestressed composite beams were mildly increased compared to that of a composite beam without tendon. The yielding loads of the prestressed composite beam with tendon were increased along with the increase in the prestressing force. However, the stiffness and yield loads of the composite beams with cover plate were sharply increased compared to that of the prestressed composite beam with tendon, as shown in Fig. 18. The yielding loads of the prestressed composite beam with cover plate increased with an increase in the heating temperature of the cover plate, similar to the tendon case. However, the ultimate strengths of the prestressed composite beams were shown to be the same regardless of the prestressing force used for the same prestressing member.

Tables 8 and 9 compare the effect of the prestressing force and the prestressing member on the prestressed composite beam. In Tables 8 and 9, the yield load of the prestressed composite beam is defined as the load at the yield stress of the lower side of the bottom flange. Ratio A is the yield load increase ratio as the prestressing force, ratio B is the sectional effect in the total prestressing effect, and ratio C is the prestressing force effect in the total prestressing effect.

For prestressing using tendon, as shown in Table 8, the sectional effect that depended on the tendon reached 3% of the yield load of the composite beam, which was not prestressed. In addition, the results show that as the prestressing force increased, so did the yield load, although the yield load did not increase in proportion to the increase in the prestressing force. We also estimated that the effect of the prestressing force by tendon was 82.2~88.0% of the total prestressing effect. Therefore, in the case of the prestressed composite beam with tendon, the effect of the prestressing force is more dominant than the effect of the section increase due to the tendon in the load-carrying

Table 8 Load-carrying capacity and the ratios according to the prestressing force level

	w/o strand	Prestressing force			
		0 kN	180 kN	360 kN	540 kN
Yield load (kN)	332.85	342.84	389.10	405.20	415.80
Ratio A	1.000	1.030	1.169	1.217	1.249
Ratio B	-	1.000	0.177	0.138	0.120
Ratio C	-	0.000	0.822	0.862	0.880

*Ratio A=Each case / w/o strand : yield load increase ratio as prestressing level

*Ratio B=(non-prestressed case w/ strand – w/o strand)/(each prestressed case – w/o strand): sectional effect in total prestressing effect

*Ratio C=1-Ratio B=prestressing force effect in total prestressing effect

Table 9 Load-carrying capacity and the ratios according to the temperature distribution level

	w/o cover-plate	Temperature distribution level			
		0-0-0°C	30-50-30°C	60-100-60°C	90-150-90°C
Yield load (kN)	332.85	554.51	625.91	682.58	732.98
Ratio A	1.000	1.666	1.880	2.051	2.202
Ratio B	-	1.000	0.756	0.634	0.554
Ratio C	-	0.000	0.244	0.366	0.446

*Ratio A=Each case / w/o strand : yield load increase ratio as temperature distribution level

*Ratio B=(non-prestressed case with cover-plate – w/o cover-plate)/(each prestressed case – w/o cover-plate): sectional effect in total prestressing effect

*Ratio C=1-Ratio B=prestressing force effect in total prestressing effect

capacity of the prestressed composite beam with tendon increase.

For prestressing using a cover plate, as shown in Table 9, the sectional effect of the cover plate on the yield load of the composite beam with cover plate reached 66.6% of the yield load of the composite beam without a cover plate compared to the effect of the composite beam where prestressing was induced. The prestressing effect on the yield load of the prestressed composite beam with cover plate increased along with an increase in temperature distribution. The prestressing effect by the change in temperature distribution of the cover plate was shown to increase in proportion to the prestressing force compared to the prestressed composite beam with tendon. We also estimated that the prestressing force effects of the cover plate were 24.4~44.6% of the total prestressing effect when cooling the heated cover plate. At the lower temperature distribution, the sectional effect of the increase in yield load was more dominant, but the prestressing effect for the increase in the yield load was more dominant in the case of higher temperature distribution.

From the FE analysis, a comparison of the load-deflection relationship for the non-prestressed composite beam showed that the load-carrying capacity of the prestressed composite beam is increased by the prestressing force and the installed prestressing member. However, the ultimate strength of the prestressed composite beam was not increased according to the increase in the prestressing force; the ultimate strength was shown to be same level. This can be explained by the plastic resistance moment of the composite section and prestressing member. The ultimate strength of the prestressed composite beam can be calculated according to the plastic neutral axis and plastic

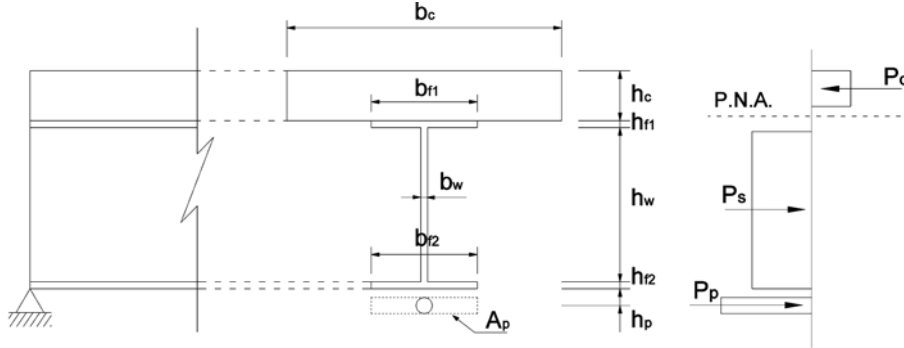


Fig. 19 Stress distribution for the plastic neutral axis in the concrete element

resistance area.

In the case of the plastic neutral axis in the concrete element, as shown in Fig. 19, the depth of the compressed element of concrete c can be calculated using Eq. (6). The depth between the compressed element of the concrete and the tensile element of steel is z . The ultimate resistance moment of the composite girder M_u can be determined using Eq. (7). When prestressing is applied to a composite girder, z is changed by the prestressing member, and the ultimate resistance moment of the composite girder is increased by the increase in the plastic resistance area according to the installed prestressing member. Therefore, the ultimate resistance moment of the prestressed composite girder M_{u-p} and the depth between the plastic neutral axis and the compressed element of concrete is determined using Eq. (8) and Eq. (9). The ultimate resistance moment of the prestressed composite girder is increased.

$$c = \frac{A_s f_{yd}}{b_c f_{ck}} \quad (6)$$

$$\begin{aligned} M_u &= P_c \cdot z = P_s \cdot z \\ &= P_c \cdot (y_{cz} + y_{sz}) = P_s \cdot (y_{cz} + y_{sz}) \end{aligned} \quad (7)$$

$$c_p = \frac{A_s f_{yd} + A_p f_{yd-p}}{b_c f_{ck}} \quad (8)$$

$$\begin{aligned} M_{u-p} &= P_c \cdot y_{cz-p} + P_s \cdot y_{sz-p} + A_p f_{yd-p} \cdot y_{tz-p} \\ &= P_c \cdot y_{cz-p} + P_s \cdot y_{sz-p} + P_p \cdot y_{tz-p} \end{aligned} \quad (9)$$

where, P_c is the compressive strength of concrete slab, P_s is the tensile strength of the steel girder, P_p is the tensile strength of the prestressing member, y_{cz} is the distance between the plastic neutral axis and P_c , y_{sz} is the distance between the plastic neutral axis and P_s , y_{cz-p} is the distance between the changed plastic neutral axis and P_c , y_{sz-p} is the distance between the changed plastic neutral axis and P_s , y_{tz-p} is the distance between the changed plastic neutral axis and P_p , A_s is the area of a steel girder, f_{yd} is the yield stress of a steel girder, A_p is the area of the prestressing member, and f_{yd-p} is the yield stress of the prestressing member.

In the case of the plastic neutral axis in the top flange or web of the steel beam, as shown in Fig. 20, the depth of the tensile element of steel S_{f-p} and S_{w-p} are derived using Eq. (10) and Eq. (11)

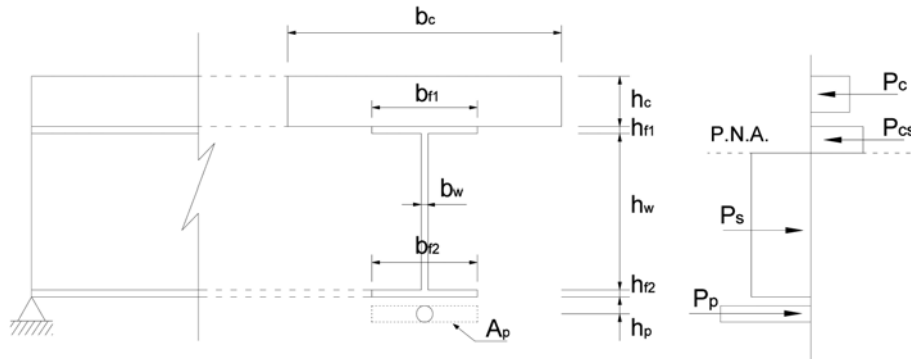


Fig. 20 Stress distribution for the plastic neutral axis in the top flange or web of the steel beam

from the plastic resistance relationship of the compressive element and tensile element. The ultimate resistance moment of the prestressed composite beam can be determined using Eq. (12).

$$s_{f-p} = \frac{A_s f_{yd} + A_p f_{yd-p} - A_c f_{ck}}{2 b_f f_{yd}} \quad (10)$$

$$s_{w-p} = \frac{A_s f_{yd} + A_p f_{yd-p} - A_c f_{ck} - 2 h_{f1} b_f f_{yd}}{2 b_w f_{yd}} \quad (11)$$

$$\begin{aligned} M_{u-p} &= P_c \cdot y_{cz-p} + P_{cs} \cdot y_{csz-p} + P_s \cdot y_{sz-p} + A_p f_{yd-p} \cdot y_{tz-p} \\ &= P_c \cdot y_{cz-p} + P_{cs} \cdot y_{csz-p} + P_s \cdot y_{sz-p} + P_p \cdot y_{tz-p} \end{aligned} \quad (12)$$

where P_{cs} is the compressive strength of the steel element and y_{csz-p} is the distance between the changed plastic neutral axis and P_s .

The ultimate strength, which is calculated using the ultimate strength equations of the prestressed composite beam, is presented in Table 10. In Table 10, the ultimate strength of the prestressed composite beam with cover plate is shown to have increased to 161% of the non-prestressed composite beam, and in the case of the prestressed composite beam with tendon, a 3% increase is shown. This is because the sectional effect of the cover plate on the composite beam is larger than that of the tendon, and this result is similar to the increased ratio in the yield load of the prestressed composite beam from the FE analysis.

Therefore, it can be confirmed that the prestressing force induced by the prestressing member increases the load-carrying capacity and the installed prestressing member increases the ultimate

Table 10 Ultimate loads and ratios of the prestressed composite beam

	Composite beam w/o the prestressing member	Prestressed composite beam	
		Strand	Cover-plate
Ultimate load (kN)	356.7	367.8	573.6
Ultimate resistance moment (kN·m)	802.51	827.50	1290.55
Ratio	1.00	1.03	1.61

*Ratio=Each case / Without the prestressing member

strength of the composite beam. In the case of the prestressed composite beam with tendon, this prestressing method can be useful in strengthening the composite beam without an increase in the self-weight of the composite beam in order to improve the load-carrying capacity of the existing bridge. In the case of the prestressed composite beam with cover plate, this prestressing method can be useful in reducing the deflection of the composite beam and strengthening the composite beam by inducing prestress, when a large deflection can occur due to the insufficiency of the section properties of the composite beam by applying the tendon to strengthen the composite beam.

6. Conclusions

This study was performed to evaluate the behavioral characteristics of prestressed composite beams to which different prestressing forces and prestressing members are applied. For this objective, the prestressed composite beams using the tendon and cover plate for thermal prestressing were fabricated and the experimental results were compared. An FE analysis and analytical analysis of the prestressed composite beam were carried out to evaluate the prestressing effect resulting from the installed prestressing member and the prestressing force. The results of this study are as follows.

From the static loading test of the prestressed composite beam with prestressing member, the prestressed composite beam specimens with tendon were increased by 16~19% of the yield load and by 1~5% of the stiffness of the composite beam. The prestressed composite beam specimens with cover plate were increased by 76~91% of the yield load and by 40~55% of the stiffness of the composite beam, depending on the connection detail. In the case of the prestressing method using tendon, the contribution of the section increase to the improvement in the load-carrying capacity of the prestressed composite beam was less than that of the inducing prestressing force, similar to about 3% of the yield load of the non-prestressed composite beam without tendon. However, in the case of the prestressing method using cover plate, the effect on improvement in the load-carrying capacity of the prestressed composite beam was shown to be larger than the case with the tendon depending on the sectional increase by the installed cover plate. The prestressing force effects of the cover plate were 24.4~44.6% of the total prestressing effect depending on the cooling of the heated cover plate from the FE analysis. The ultimate strength of the prestressed composite beam was shown to be same value because ultimate strength is determined according to the plastic resistance moment relation affected by the plastic neutral axis and plastic resistance area, regardless of the prestressing force. Therefore, the prestressing method using prestressing member can increase the load-carrying capacity of the composite beam and less deflection can be achieved in the serviceability state.

From this study, the prestressing method using tendon can be useful to strengthen the composite beam without an increase in composite beam weight. The prestressing method using cover plate can be applied to reduce the deflection of the composite beam as well as to strengthen the composite beam by inducing prestress when there is a large deflection due to the insufficiency of the section properties of the composite beam.

Acknowledgements

This study has been supported by Seunghwa Engineering & Construction. This study also has

been supported in part by Yonsei University, Center for Future Infrastructure System, a Brain Korea 21 program, Korea.

References

- Ahn, J.H., Jung, C.Y., Kim, J.H. and Kim, S.H. (2009), "Multi-stepwise thermal prestressing using a cover-plate in steel structures", *J. Constr. Steel Res.*, **65**, 1464-1479.
- Ahn, J.H., Jung, C.Y., Choi, K.T. and Kim, S.H. (2009a), "Plate girder bridge strengthened with multi-stepwise thermal prestressing method", *Adv. Struct. Eng.* (in review).
- Ahn, J.H., Jung, C.Y., Choi, K.T. and Kim, S.H. (2009b), "Load-carrying capacity evaluation of the composite beam strengthened by multi-stepwise thermal prestressing method using cover-plate", *J. Korea Inst. Struct. Maint. Inspection* (in press).
- Chen, S. and Gu, P. (2005), "Load carrying capacity of composite beams prestressed with external tendons under positive moment", *J. Constr. Steel Res.*, **61**, 515-530.
- Fisher, J.W. and Wright, W.J. (2001), "High performance steel enhanced the fatigue and fracture resistance of steel bridge structures", *Int. J. Steel Struct.*, **1**(1), 1-7.
- Korea Highway Bridge Specifications (2005), *Korean Ministry of Construction and Transportation*.
- Lorenc, W. and Kubica, E. (2006) "Behavior of composite beams prestressed with external tendons: experimental study", *J. Constr. Steel Res.*, **62**(12), 1353-1366.
- Oehlers, D.J., Nguyen, N.T., Ahmed, M. and Bradford, M.A. (1997), "Partial interaction in composite steel and concrete beams with full shear connection", *J. Constr. Steel Res.*, **41**(2/3), 235-248.
- Queiroz, F.D., Vellasco, P.C.G.S. and Nethercot, D.A. (2007), "Finite element modeling of composite beams with full and partial shear connection", *J. Const. Steel Res.*, **63**, 505-521.
- Ranzi, G. and Bradford, M.A. (2009), "Nonlinear analysis of composite beams with partial shear interaction by means of the direct stiffness method", *Steel Compos. Struct.*, **9**(2), 131-158.
- Sakano, M., Namiki, H., Yajima, S., Koide, Y. and Furuta, H. (2006) "Frangopol DM. Monitoring of steel railway floor beams prestressed by steel plates", *J. Bridge Eng.*, **11**(6), 681-687.

Appendix

A. General application procedure of the prestressing method using cover plate (multi-stepwise TPSM)

As illustrated in Fig. 21(a), a cover plate is heated with electric heaters prior to attachment to the beam. The insulators are installed to particularly prevent heat transfer from the cover plate to the steel beam and to minimize heat loss on the opposite side where the induction heater is installed in the prestressing with the cover plate. After thermal equilibrium is reached (no further temperature change), the cover plate is connected to the beam using high tension bolts at the anchorages after insulators are removed, as shown in Fig. 21(b). After bolting is completed, the heaters are removed and the contraction behavior of the cover plate, as it is cooled, induces prestresses in the beam. By differentiating the heating temperature between bolted anchorages, the prestress due to thermal prestressing shows a multi-stepwise distribution, as illustrated in Fig. 21(c).

B. Heating system for the prestressing method using cover plate (multi-stepwise TPSM)

The heating system of the multi-stepwise TPSM should be able to heat the cover plate in a short period of time and thereby guarantee a uniform relative temperature difference between the atmospheric temperature and the cover plate. Fig. 22 is a heating system developed for this purpose and is composed to an induction-type heater with an automatic controller to uniformly maintain the relative temperature difference between the atmospheric temperature and the cover plate.

The induction-type heater is a very safe device that uses an electromagnetic field in contrast to a general heating system that transfers heat energy from itself to the material to be heated. The automatic controller with a thermocouple that measures the temperatures of the bridge and cover plate maintains the uniform relative temperature difference between them.

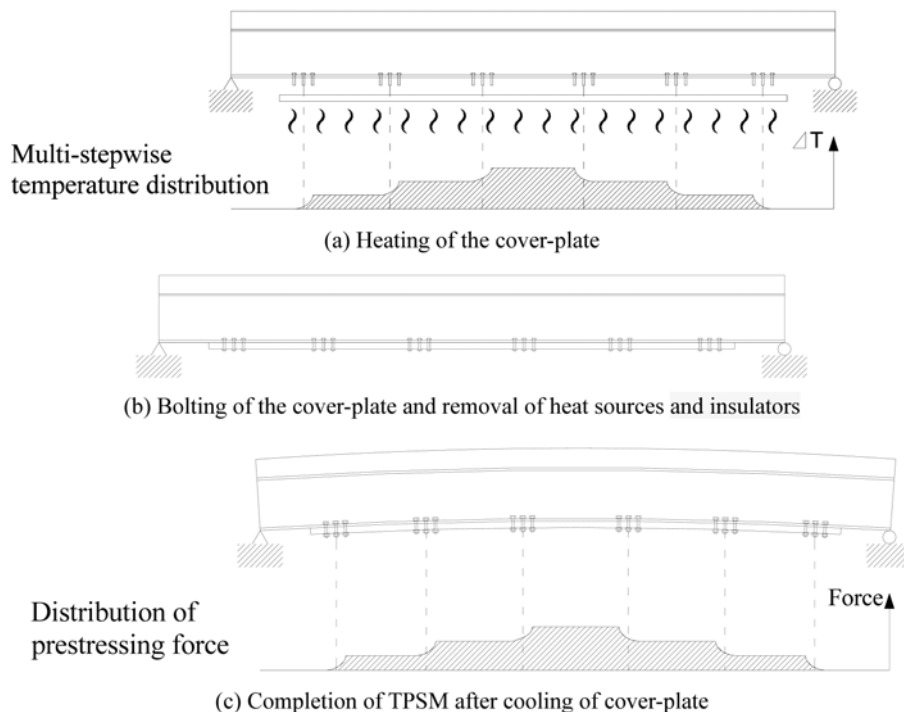
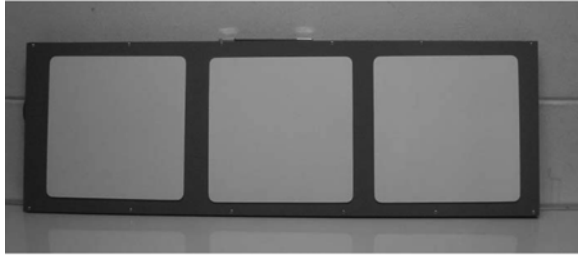


Fig. 21 General procedure of the prestressing method using cover-plate (multi-stepwise TPSM)



(a) Induction-type electric heater



(b) Automatic controller

Fig. 22 Induction-type heating system